

Atomic and ionic processes of silicon oxidation

A. Marshall Stoneham,^{1,*} Marek A. Szymanski,^{1,2} and Alexander L. Shluger¹

¹Centre for Materials Research, Department of Physics and Astronomy, University College London, Gower Street, London WC1E 6BT, United Kingdom

²Faculty of Physics, Warsaw University of Technology, ulica Koszykowa 75, 00-662 Warsaw, Poland

(Received 20 February 2001; published 7 June 2001)

Our state-of-the-art calculations for ionic and neutral oxygen species, both molecular and atomic, in amorphous silicon dioxide show the amorphous nature of the oxide changes significantly the energetics of defect processes like charge state change, incorporation into the oxide network, and splitup of the molecule. These changes imply a new picture of silicon oxidation in the ultrathin film regime that explains anomalies like layer-by-layer growth at terraces, roughness oscillations, the distribution of oxygen isotope incorporation, the effects of excitation, and deviations from Deal-Grove kinetics. Our results suggest possible alternative routes to improve oxide quality.

DOI: 10.1103/PhysRevB.63.241304

PACS number(s): 81.65.Mq, 66.30.Lw, 71.23.-k, 71.55.Ht

The oxide on silicon is a major factor in silicon's domination of microelectronics: the outstanding gate dielectric, it passivates the Si surface, and can be exploited in processing. Yet there is a looming "doomsday scenario": no means is known to meet the dielectric reliability targets in the semiconductor industry roadmap. Nor are alternative dielectrics likely to be available in time. So, are there new ways to squeeze extra performance from silicon's oxide? Understanding the key oxide growth processes is surely essential, going beyond average oxide structures and empirical or incremental experimental studies. One must understand certain "problem features":¹ layer-by-layer growth² at terraces,³ roughness oscillating with oxide thickness,⁴ the distribution of oxygen isotope incorporation,⁵ effects of excitation,⁶ systematic deviations from reaction-diffusion kinetics (Deal-Grove model)¹ and effects of electron injection.⁷ Our state-of-the-art electronic structure theory for α quartz^{8,9} and Monte Carlo calculations¹⁰ go beyond standard models by considering atomic and molecular oxidizing species, charged and neutral, and processes associated with the Si/oxide interface. Our results here for the *amorphous oxide* rationalize the "problem features" and suggest alternative approaches to oxide control and optimization.

The oxide on silicon is amorphous. Favored sites provide explanations of oxygen solubility¹¹ and hole self-trapping. To have a representative model, we have generated a number of periodic 72-atom amorphous structures by quenching from a melt using a well-tested set of two- and three-body empirical potentials.¹² The unit cell was constructed to match the experimental density. Each quenched structure was then fully relaxed (atomic positions and lattice vectors) using VASP code^{13,14} with state-of-the-art density functional theory (DFT), described below. The DFT relaxation energies and displacements were homogeneous and very small (less than 0.02 eV per atom, including the small volume change), implying that the potentials gave good initial geometries. All the amorphous models have been characterized, and show very good agreement with experimental data and with previous calculations of bigger systems for properties such as energy per molecular unit, pair distribution function, angular distribution function, and ring statistics. To test the stability

of the structures we ran 0.5 ps DFT molecular dynamics (MD) calculation at 600 K, for which the average rise in potential energy of the supercell was 5.5 eV. The systems did not leave their minima of energy; and quenching to 0 K (by geometry relaxation) recovered the same structures. The characterization of our samples indicates that the structures should be usefully representative of amorphous (a)-SiO₂ for their density.

The structure with the lowest energy was chosen for detailed study of atomic and molecular oxygen species inside growing oxide. The quench rate for this structure was 100 K/16 ps and the total time of quench was 360 ps. The relaxed supercell is almost cubic with lattice vectors lengths of 10.07, 10.61, and 10.06 Å. The density of the sample is 2.23 g/cm³ compared with experimental density of 2.20 g/cm³. We note, however, that the DFT method used in this work tends to underestimate the density by few percent for SiO₂ structures and that amorphous silicas can have wide range of densities depending on the way they were formed. The structure of the real oxides on silicon is unsettled, and appears to vary somewhat depending on the precise oxidizing conditions. We have not attempted to model structure variations through the oxide thickness. Our calculations are, therefore, for reference amorphous oxides similar in density to real oxides. The average interatomic distances (evaluated over 1 ps DFT MD run at 300 K after equilibration for 1 ps) are 1.643, 2.665, and 3.059 Å for Si-O, O-O and Si-Si, respectively. The average angles are 109.43° for \angle Si-O-Si and 141.38° for \angle O-Si-O. The ring statistics compares very well with previous published work, however the three- and four-membered rings are slightly over-represented at the expense of eight-membered rings.

We identified a range of promising sites for interstitial oxygens. For molecular species, we selected five of the larger interstices; molecules at two of these relaxed to other interstices, leaving three distinct local minima. For atomic species, where peroxylike linkages occur (see Table I), we chose seven Si-O-Si units to sample the bond-angle distribution. The statistical analysis of results for all interstitial sites will be published separately.

TABLE I. Average energies for different species in a-SiO₂. Atomic geometries show typical stable configurations. Positive incorporation energies E_{inc} mean endothermic incorporation from the gas phase. Positive vertical electron affinities E_{aff} mean exothermic capture of an electron from the bottom of the bulk Si conduction band. Doubly negative species show no electron affinity. The site-to-site spread of values is shown in curly brackets { }. Values for quartz (Ref. 9) are given in square brackets [].

| | Atomic geom. | Isotope exch. | E_{inc} (eV) | E_{aff} (eV) |
|---------------|--------------|---------------|--------------------|-------------------|
| O_{2i}^0 | | No | 0.4 {0.4} [2.1] | 0.2 {0.2} [0.7] |
| O_{2i}^- | | No | -1.2 {0.1} [-0.5] | -1.1 {0.2} [-0.2] |
| O_{2i}^{2-} | | No | -2.1 {0.1} [-1.9] | No affinity |
| O_i^0 | | Yes | 1.9 {0.7} [2.0] | -0.4 {0.2} [-0.5] |
| O_i^- | | Yes | -0.9 {0.7} [-0.7] | 0.0 {0.5} [-0.3] |
| O_i^{2-} | | Yes | -2.75 {0.5} [-2.8] | No affinity |

To calculate stable structures, incorporation energies and electron affinities of oxygen species, we use the spin-polarized version of the same DFT method with the generalized gradient approximation and the PW91 functional,¹³ and a plane-wave basis set with a 400 eV cutoff energy implemented within the VASP code.¹⁴ We include the Γ -point only in Brillouin-zone integration. Ultrasoft pseudopotentials were used for oxygen, and norm-conserving pseudopotentials for the silicon atoms. Defects are separated by more than 1 nm in our large unit cell. Geometry relaxation exploited conjugate gradient (CG) energy minimization, using the ascending and descending valley points to search for transition states.⁹ All relaxation procedures continued until forces on atoms were less than 0.05 eV/Å. In calculating energies of charged species in a periodic model, we use a neutralizing background to converge Ewald summations, correcting errors in the total energy to first order by the Makov-Payne monopole-monopole energy correction.¹⁵

In calculations of electron affinities of oxygen species, electrons added or removed from the system are transferred to or from the bottom of silicon conduction band at the Si/SiO₂ interface; the energies are readily adjusted if doping, temperature, or bias favor another source. The method implemented in the VASP code keeps the energy zero as a reference level, which stays at the same position with respect

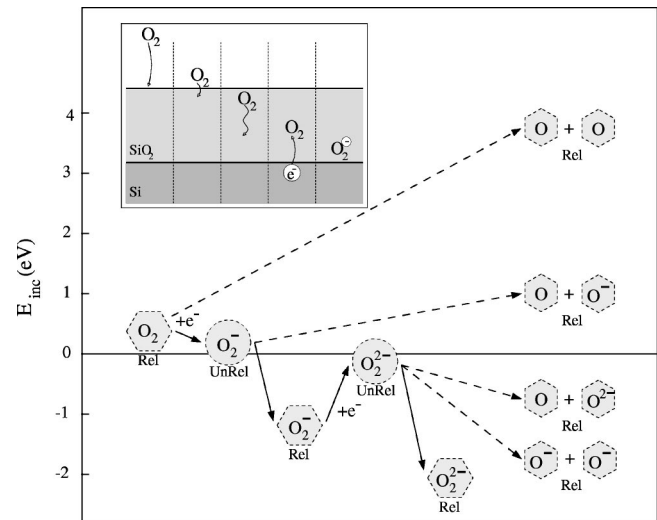


FIG. 1. Average incorporation energies for different oxidizing species in a-SiO₂ (see Table I for the spread of values). Hexagons show energies after geometry relaxation; circles show energies after electron capture before relaxation. Electrons are assumed to come from the bottom of the Si conduction band. The inset shows examples of the main oxidation steps.

to the SiO₂ valence band in all calculations. This allows reliable comparison of different charge states and means that our results correspond effectively to an isolated point defect in an infinite nondefective host lattice (a shift of the host lattice levels after incorporation of a defect would mean that the properties of the whole system are affected, whereas no shift indicates that all of the system but the local region around defect behaves as a nondefective host lattice). We use experimental information¹⁶ (4.6 eV for the valence-band offset at the Si/SiO₂ interface, 1.1 eV for the band gap of Si) to estimate the energy of an electron at the bottom of the conduction band of Si with respect to the theoretical zero energy level.

Table I and Fig. 1 give results for the lowest-energy spin state for each species. Incorporation energies relate the energy of the most stable configuration to that of the initial nondefective amorphous structure, an isolated oxygen molecule or half molecule in triplet state and the energy of electron(s) as appropriate at the bottom of the Si conduction band. Vertical electron affinities are for fixed atom positions on adding an electron. Double-negative species show no electron affinity. We show average values and their spread over the different sampled sites in the amorphous model, plus values for α quartz.

The *incorporation energies* show molecular species are more stable than atomic species, in line with earlier views. Oxygen atoms form molecules exothermically if, under oxidation conditions, there are other O with which to react. For a-SiO₂, it costs 3.8 eV to incorporate two interstitial atomic oxygens, and 0.4 eV for O_{2i}^0 , so 3.4 eV is needed to dissociate the interstitial molecule (note that this significantly less than bonding energy of a free molecule). Incorporation of neutral and singly charged molecular species into a-SiO₂ needs on average 1.7 eV and 0.7 eV less energy, respec-

tively, than their incorporation into α quartz.⁸ Qualitatively, larger interstices give lower energies, providing special sites for solubility.¹¹ Clearly, α quartz can be a poor oxide mimic for reproducing average energies, especially for molecular species. Nor does α quartz have the site-to-site variations in energy and cannot give an estimate of spreads of values. Fuller calculations, to be described elsewhere, show there are significant contributions to the energies associated with medium range order not represented in the case of a crystalline host lattice or calculations with standard cluster models.

Charged species tend to be more stable than neutral species when electrons are available from the bottom of the bulk Si conduction band. Even for doubly charged species, both spin and charge seem well localized on the species itself. Incorporation energies fall as negative charge increases: charging could be relatively common, although cases like $O_{2i}^- + e^- \rightarrow O_{2i}^{2-}$ may proceed by inelastic tunneling capture.¹⁷ In a-SiO₂, the electron affinity (and hence electron capture probability) varies from site to site. Oxide polarization is partially included in supercell calculations, and the terms omitted will favor charged species. Si substrate polarization¹⁸ (not included here) also favors localized charges.

Our predictions thus suggest a significant role for charged interstitial oxygens, which supports many previous experimental claims,¹⁹ including the effects on oxidation kinetics of bias voltages and of ultra-low-energy electrons.¹⁰ Plasma oxidation kinetics follows trends expected for ionic species.²⁰ Oxygen adsorption on SiO₂ results in O_{2i}^- species.²¹ Telegraph noise²² requires charge transfer between Si and its oxide.

There are reactions which are either exothermic or approximately energy neutral in which interstitial molecules (relaxed initially) dissociate on electron capture: O_{2i}^- can simply relax to O_{2i}^{2-} , but could split into $2O_i^-$; the latter process is less likely, partly because the relaxation energy is less, and partly because the two ions might recombine. An initially-neutral molecule, on capturing an electron by tunneling, may split into $O_i^0 + O_i^-$, but this is marginal energetically. It is not enough, however, to know the minimum energy properties of the species to judge the contribution of atomic species to silicon oxidation. The detailed knowledge of diffusion mechanisms is required too. For example, the doubly bonded structure of O_{2i}^{2-} is likely to have a high diffusion barrier. Transport may be more effective by dissociation into $2O_i^-$ which then diffuse as two separate ions.

In addition to minimum energy structures (see Table I) we first calculated the diffusion paths and diffusion barriers for all the species in α quartz.⁹ The stable structures in amorphous and crystalline host lattice are similar and we should expect the diffusion mechanisms to be also analogous. On this basis we conclude that the structures and diffusion of atomic species (O_i^0 , O_i^- , O_i^{2-}) in a-SiO₂ involve incorporation of O into the oxide network and easy isotope exchange with network oxygens. The structures and diffusion mechanisms of molecular species (O_{2i}^0 , O_{2i}^- , O_{2i}^{2-}) make significant isotope exchange unlikely, except at special network sites or substoichiometric regions, such as those proposed near the Si/oxide interface in the reactive-layer model. Since

observed isotope exchange is concentrated near the oxide interfaces, atomic interstitial oxygen can only be significant near these interfaces. When excitation by low-energy electrons⁷ creates atomic species, exchange occurs throughout the oxide, as expected.

Very low diffusion motion energies are predicted for O_{2i}^0 in α quartz, of order 0.1 eV.^{8,9} In a-SiO₂, energies will be higher because available diffusion paths must sample the low-energy sites and a distribution of barriers. The average value of the measured activation energy for oxygen diffusion is about 1.2 eV, with a significant spread.²³ The barriers for molecular diffusion relate to sizes of passages. We have made initial calculations of the barriers through rings of different sizes in the amorphous oxide (a fuller analysis will be published separately). Values of the barriers relative to the mean of incorporation energies for the interstitial molecules are over 2.3 eV for five-membered rings, 1.6–2.4 eV for six-membered rings, and around 1.2–1.3 eV for seven-membered rings. Examination of the amorphous topology shows, on average about two seven-membered rings and three six-membered rings involved in building each big void. The 1.2–1.3 eV diffusion energy for seven-membered rings agrees well with the experimental value. The activation energy for oxidation should be higher than the diffusion energy by 0.4 eV (average incorporation energy for the oxygen molecule); again the prediction of about 1.6–1.7 eV is fully consistent with experiment (1.3–2.3 eV).

Our results suggest a new picture of silicon oxidation, arising from the atomic and charged species created by tunneling near the Si/oxide interface. Assume, consistent with our results for a-SiO₂ that charged molecular and atomic oxygen species can be created in the oxide within an electron tunneling distance (say 1 nm) of the Si/oxide interface. First, Monte-Carlo calculations^{1,10} show charged oxidizing species explain the “problem features” (layer-by-layer growth on terraces, deviations from Deal-Grove for ultrathin oxides, etc.) phenomenologically. Silicon is more polarizable than its oxide, and the polarization energy biases key steps. Secondly, these charged species will be far less important for thick oxide, where diffusion of neutral oxygen molecules (as in Deal-Grove) remains the main rate-determining process. Our results for O_{2i}^0 in amorphous oxide lead to an energy of oxidation similar to that observed. Thirdly, even for thick oxides, isotope incorporation will indicate where atomic species are formed. If they are formed during capture of electrons tunneling from the Si, one expects exchange primarily near the Si/oxide interface (a reactive layer²⁴ may not be needed). Fourthly, our results are consistent with the observed effects of low-energy electrons, both on kinetics and on isotope incorporation. Finally, we stress that α quartz is not a good oxide model for oxidation processes: an amorphous oxide is crucial.

Existing oxide dielectric reliability data fit a picture which involves creating random oxide defects until a conducting channel of overlapping defects forms.^{25,26} For the thinnest oxides, even one defect might be problematic. One critical defect for stress-induced leakage currents²⁷ is credibly believed to be the H bridge,²⁸ with H associated with an intrinsic defect. Reliability requires oxide fine-tuning to eliminate

damaging or vulnerable features. Such features might be point defects, perhaps initiated as Si/oxide interface defects,²⁹ or topological defects. Defects like O vacancies will react readily with atomic or molecular oxygen. Other defects may react directly with O_{2i} only with difficulty, since two oxygens must find suitable sites. An example might be an Si-Si bond [not an O vacancy, but a direct Si-Si bond in the oxide, like that inferred from oxygen hyperfine data as part of the P_b center on Si(111) (Ref. 30)]. Yet a single O_i in an appropriate charge state could render the vulnerable feature harmless. Given the different behaviors predicted for atomic and molecular species, *control of the proportions of atomic and molecular species* (whether by a mix of oxygen with ozone or by providing some atomic oxygen) *offers one route to improvements in reliability.*

Control of charge state might be even more important for very thin oxides, through two distinct effects. Making Si the cathode encourages electron emission, creating charged species close to the Si/oxide interface. Making Si the anode

biases ionic diffusion and the spatial distribution of the different charge states. These processes have different time scales. *It is likely that oxide quality can be improved by a sequence of applied electric fields with well-chosen magnitudes, directions and durations controlling the populations of different oxidising species at the interface.* Identifying the potential for oxide improvement by applied electric fields and by control of atomic/molecular proportions is not yet a recipe. There is a complex interplay between the several processes. But we have identified important atomistic mechanisms which are not usually considered and which suggest new control parameters for enhancing oxide quality. In the context of the “doomsday scenario,” this understanding points to an opportunity.

We gratefully acknowledge the support of this work by the Fujitsu European Center for Information Technology, Fujitsu Laboratories, and EPSRC.

*Email address: a.stoneham@ucl.ac.uk

- ¹C. J. Sofield and A. M. Stoneham, *Semicond. Sci. Technol.* **10**, 215 (1995).
- ²V. D. Borman, E. P. Gusev, Y. Y. Lebedinskii, and V. I. Troyan, *Phys. Rev. Lett.* **67**, 2387 (1991).
- ³F. Ross and M. Gibson, *Phys. Rev. Lett.* **68**, 1782 (1992).
- ⁴T. Hattori, H. Nohira, Y. Teramoto, and N. Watanabe, in *Structure and Electronic Properties of Ultra Thin Dielectric Films on Silicon and Related Structures*, edited by D. A. Buchanan, A. H. Edwards, H. J. Bardeleben, and T. Hattori, *Materials Research Soc. Symposium Proc. 592* (Materials Research Society, Pittsburgh, 2000), p. 33.
- ⁵F. Rochet, S. Rigo, M. Froment, C. d’Anterrosches, C. Maillot, H. Roulet, and G. Dufour, *Adv. Phys.* **35**, 237 (1986).
- ⁶A. Kazor and I. W. Boyd, *J. Appl. Phys.* **75**, 227 (1994).
- ⁷P. Collot, G. Gautherin, B. Agius, S. Rigo, and F. Rochet, *Philos. Mag. B* **52**, 1051 (1985).
- ⁸A. M. Stoneham, M. A. Szymanski, and A. L. Shluger, in *Structure and Electronic Properties of Ultrathin Dielectric Films on Silicon and Related Structures*, *MRS Symp. Proc.* **592**, 3 (2000) (Ref. 4, p. 3).
- ⁹M. A. Szymanski, A. M. Stoneham, and A. L. Shluger, *Solid State Electron.* (to be published).
- ¹⁰V. J. B. Torres, A. M. Stoneham, C. J. Sofield, A. H. Harker, and C. F. Clement, *Interface Sci.* **3**, 131 (1995).
- ¹¹N. F. Mott, S. Rigo, F. Rochet, and A. M. Stoneham, *Philos. Mag. B* **60**, 189 (1989).
- ¹²P. Vashishta, R. K. Kalia, J. P. Rino, and I. Ebbsjö, *Phys. Rev. B* **41**, 12 197 (1990).
- ¹³J. P. Perdew, J. A. Chevary, S. H. Vosko, K. A. Jackson, M. R. Pederson, D. J. Singh, and C. Fiolhais, *Phys. Rev. B* **46**, 6671 (1992).
- ¹⁴G. Kresse and J. Furthmüller, *Phys. Rev. B* **54**, 11 169 (1996).
- ¹⁵V. Makov and M. C. Payne, *Phys. Rev. B* **51**, 4014 (1995).
- ¹⁶J. L. Alay and M. Hirose, *J. Appl. Phys.* **81**, 1606 (1997).
- ¹⁷W. B. Fowler, J. K. Rudra, M. E. Zvanut, and F. J. Feigl, *Phys. Rev. B* **41**, 8313 (1990).
- ¹⁸A. M. Stoneham and P. W. Tasker, *Philos. Mag. B* **55**, 237 (1987).
- ¹⁹D. R. Wolters and A. T. A. Zegers-van Duijnhoven, *J. Electrochem. Soc.* **139**, 241 (1992).
- ²⁰C. Martinet, R. A. B. Devine, and M. Brunel, *J. Appl. Phys.* **81**, 6996 (1997).
- ²¹N. Shamir, J. M. Mihaychuk, and H. M. van Driel, *Phys. Rev. Lett.* **82**, 359 (1999).
- ²²M. J. Kirton and M. J. Uren, *Adv. Phys.* **38**, 367 (1989).
- ²³M. A. Lamkin, F. L. Riley, and R. J. Fordham, *J. Eur. Ceramic Soc.* **10**, 347 (1992).
- ²⁴A. M. Stoneham, C. R. M. Grovenor, and A. Cerezo, *Philos. Mag. B* **55**, 201 (1987).
- ²⁵R. Degraeve, G. Groeseneken, R. Bellens, M. Depas, and H. E. Maes, in *IEDM95* (IEEE, New York, 1995), p. 863.
- ²⁶D. J. DiMaria, *Microelectron. Eng.* **36**, 317 (1997).
- ²⁷D. J. DiMaria and E. Cartier, *J. Appl. Phys.* **78**, 3883 (1995).
- ²⁸P. E. Blöchl and J. H. Stathis, *Phys. Rev. Lett.* **83**, 372 (1999).
- ²⁹A. M. Stoneham and C. J. Sofield, in *Fundamental Aspects of Ultrathin Dielectrics in Si Based Devices*, edited by E. Garfunkel, E. Gusev, and A. Vul’ (Kluwer, Dordrecht, 1998), p. 79.
- ³⁰C. K. Ong, A. M. Stoneham, and A. H. Harker, *Interface Sci.* **1**, 139 (1993).